Novel Hybrid Spin Systems of 7,7′,8,8′-Tetracyanoquinodimethane (TCNQ) Radical Anions and 4-Amino-3,5-bis(pyridin-2-yl)-1,2,4-triazole (abpt). Crystal Structure of $[Fe(abpt)_2(TCNQ)_2]$ at 298 and 100 K, Mössbauer Spectroscopy, Magnetic Properties, and Infrared Spectroscopy of the Series $[M^{II}(abpt)_2(TCNQ)_2]$ (M = Mn, Fe, Co, Ni, Cu, Zn)

Paul J. Kunkeler,[1a] Petra J. van Koningsbruggen,[1a] Joost P. Cornelissen,[1a] André N. van der Horst,[1b] Adri M. van der Kraan,[1b] Anthony L. Spek,[1c] Jaap G. Haasnoot,*[,1a] and Jan Reedijk[1a]

Contribution from the Leiden Institute of Chemistry, Gorlaeus Laboratories, Leiden University, P.O. Box 9502, 2300 RA Leiden, The Netherlands, Interuniversity Reactor Institute, Delft University of Technology, Delft, The Netherlands, and Bijvoet Center for Biomolecular Research, Vakgroep Kristal- en Structuurchemie, Utrecht University, Padualaan 8, 3584 CH Utrecht, The Netherlands

Received December 7, 1994. Revised Manuscript Received September 13, 1995[⊗]

Abstract: The compound $[Fe(abpt)_2(TCNQ)_2]$, where TCNQ is the radical anion 7,7′,8,8′-tetracyanoquinodimethane and abpt = 4-amino-3,5-bis(pyridin-2-yl)-1,2,4-triazole, is an Fe(II) complex containing coordinated radical anions which undergoes a thermally induced spin-crossover with $T_c = 280$ K. Variable-temperature magnetic susceptibility (7−460 K) and ^{57}Fe Mössbauer spectroscopy data give evidence for a complete $S = 2$ (high-spin) ↔ $S = 0$ (low-spin) transition, taking place gradually, without hysteresis. The X-ray structure has been determined at 298 K (**1**) and 100 K (**2**). The compound crystallizes in the triclinic space group $P\bar{1}$ with one molecule in the unit cell of dimensions $a = 9.277(2)$ Å, $b = 9.876(3)$ Å, $c = 12.272(2)$ Å, $\alpha = 69.52(2)°$, $\beta = 86.92(2)°$, and $\gamma = 81.73(2)°$ for **1** and $a = 9.236(2)$ Å, $b = 9.684(1)$ Å, $c = 12.137(2)$ Å, $\alpha = 69.26(1)°$, $\beta = 87.53(2)°$, and $\gamma = 82.38(1)°$ for **2**. Two abpt ligands coordinating *via* pyridyl-N1A and triazole-N1 are in the equatorial positions. Fe−N1 and Fe−N1A distances are 2.08(1) and 2.12(1) Å for **1** and 2.00(2) and 2.02(1) Å for **2**, respectively. TCNQ molecules coordinate axially at remarkably short distances *i.e.*, Fe−N1T = 2.16(1) Å for **1** and 1.93(1) Å for **2**. The TCNQ molecules are stacked in pairs yielding diamagnetic entities. The FT-IR spectra (100−300 K) show that the TCNQ ν_{CN} vibrations are a fingerprint for the different spin states. In the series of the isostructural $[M^{II}(abpt)_2(TCNQ)_2]$ (M = Mn, Fe, Co, Ni, Cu, Zn) compounds, the ν_{CN} absorptions show a shift to higher frequencies as a function of the crystal field stabilization energy. Above T_c, the Cu(II)-doped Fe(II) species shows a broad signal with $g_\perp = 2.09$ and $g_\parallel = 2.25$ and hyperfine structure ($A_\parallel = 180$ G). At T_c and below, the spectrum becomes better resolved and now shows superhyperfine structure ($A_{N\parallel} = 16$ G; nine lines). Above T_c, the Mn(II)-doped Fe(II) compound shows a very broad signal at $g = 2.00$. The spectrum sharpens at T_c to give a clearly resolved spectrum corresponding to a magnetically isolated Mn(II) ion in a tetragonal environment. The signal is split by the zero-field splitting, yielding major signals at $g = 1.6$ and $g = 5.5$ and six hyperfine lines ($A_\parallel = 80$ G) that are clearly visible on both signals.

Introduction

In the study of the magnetic properties of coordination compounds containing transition-metal ions, two important fields of research have attracted much attention over the past years: the study of the spin-crossover phenomenon[2] and the research on compounds containing transition-metal ions and organic radicals.[3] A variety of iron(II) compounds are known to show a transition from the high-spin state (HS, $S = 2$, $^5T_{2g}$) to the low-spin state (LS, $S = 0$, $^1A_{1g}$) on cooling,[2] upon increasing pressure,[2b,4] or by light irradiation.[5] The interest in these bistable spin-crossover compounds finds its origin in their possible use in molecular electronics, for which it would be favorable when

⊗ Abstract published in *Advance ACS Abstracts,* February 15, 1996.

(1) (a) Leiden University. (b) Delft University of Technology. (c) Utrecht University.

(2) (a) König, E.; Ritter, G.; Kulshreshtha, S. K. *Chem. Rev.* **1985**, *85*, 219. (b) Gütlich, P. *Struct. Bonding* **1981**, *44*, 83. (c) Zarembowitch, J.; Kahn, O. *New. J. Chem.* **1991**, *15*, 181−190. (d) Goodwin, H. A. *Coord. Chem. Rev.* **1976**, *18*, 293. (e) Gütlich, P. In *Mössbauer Spectroscopy Applied to Inorganic Chemistry*; Long, G. J., Ed.; Modern Inorganic Chemistry Series, Vol. 1; Plenum Press: New York, 1984. (f) Bacci, M. *Coord. Chem. Rev.* **1988**, *86*, 245. (g) König, E. *Prog. Inorg. Chem.* **1987**, *35*, 527.

(3) (a) Kahn, O.; Prins, R.; Reedijk, J.; Thompson, J. S. *Inorg. Chem.* **1987**, *26*, 3557. (b) Eaton, S. S.; Eaton, G. R. *Coord. Chem. Rev.* **1978**, *26*, 207. (c) Pierpont, C. G.; Buchanan, R. M. *Coord. Chem. Rev.* **1981**, *38*, 45. (d) Laugier, J.; Rey, P.; Benelli, C.; Gatteschi, D.; Zanchini, C. *J. Am. Chem. Soc.* **1986**, *108*, 6931. (e) Caneschi, A.; Ferraro, F.; Gatteschi, D.; Rey, P.; Sessoli, R. *Inorg. Chem.* **1991**, *30*, 3162. (f) Caneschi, A.; Gatteschi, D.; Laugier, J.; Rey, P. *J. Am. Chem. Soc.* **1987**, *109*, 2191. (g) Caneschi, A.; Gatteschi, D.; Laugier, J.; Rey, P.; Sessoli, R.; Zanchini, C. *J. Am. Chem. Soc.* **1988**, *110*, 2795. (h) Sessoli, R.; Tsai, H. L.; Schake, A. R.; Wang, S.; Vincent, J. B.; Folting, K.; Gatteschi, D.; Christou, G.; Hendrickson, D. N. *J. Am. Chem. Soc.* **1993**, *115*, 1804. (i) Caneschi, A.; Gatteschi, D.; Rey, P. *Prog. Inorg. Chem.* **1991**, *39*, 331.

0002-7863/96/1518-2190$12.00/0

the compound exhibits an abrupt transition with hysteresis at a critical temperature close to ambient temperature.[2c] Furthermore, spin transitions are believed to play an important role in biological systems; spin equilibria in certain hemeproteins have been reported to be coupled to electron transport.[6] In particular, iron(II) compounds containing substituted 1,2,4-triazole ligands have been found to show spin transitions, in several cases with hysteresis, and considerably high transition temperatures appear to be possible.[7] In general, spin-crossover behavior has frequently been observed for Fe(II) ions coordinated by two didentate chelating nitrogen-donating ligands, together with two monodentately coordinating nitrogen-donating ligands.[2,5c] In these cases, the monodentate ligands are generally in a *cis* configuration; a *trans* geometry has so far only been found for the two-dimensional compounds $[FeX_2(btr)_2](H_2O)$ (X = NCS,[7c,d] NCSe;[7g] btr = 4,4′-bis(1,2,4-triazole)). Organic radicals are widely used as spin probes in biological systems.[3b] Compounds which contain transition-metal ions in combination with coordinating organic radicals are now attracting considerable attention because of their interesting magnetic properties, arising from the spin−spin interaction between unpaired electron spins situated on the metal ion and on the radical,[3a,c−i] and discrete molecular units having a large total electron spin in the ground state have been obtained.[3g,h] On the other hand, this strategy also opens a way to prepare molecular ferromagnets.[3e,f,8] The type of organic radical we have focused our attention on is 7,7′,8,8′-tetracyanoquinodimethane (abbreviated as TCNQ). Recently, compounds of general formula $[M^{II}(abpt)_2(TCNQ)_2]$ (M = Cu, Ni, Co, Fe; abpt = 3,5-bis(pyridin-2-yl)-4-amino-1,2,4-triazole) have been reported.[9] These compounds represent one of the rare cases of the TCNQ radical anion being involved in coordination. Here we report a detailed study on the unusual spin transition in $[Fe^{II}(abpt)_2(TCNQ)_2]$, with a *trans*-$FeN_4N'_2$ chromophore. In addition, the physical properties of the isostructural Mn(II), Co(II), Ni(II), Cu(II), and Zn(II) compounds are described.

Experimental Section

Materials. Commercially available solvents and metal(II) salts were used without further purification. The ligand abpt was synthesized according to the method of Geldard and Lions[10] from 2-cyanopyridine (FLUKA A.G.) and hydrazine hydrate (Janssen Chemicals). TCNQ was obtained from Janssen Chemicals. LiTCNQ was prepared by adding a boiling solution of 0.03 mol of LiI in 20 mL of acetonitrile to a boiling solution of 0.01 mol of TCNQ in 200 mL of acetonitrile. Dark purple microcrystals precipitated.[11]

Synthesis of $[M^{II}(abpt)_2(TCNQ)_2]$ (M(II) = Mn(II), Fe(II), Co(II), Ni(II), Cu(II), Zn(II)). The complexes were prepared according to a modification of the method described by Cornelissen.[9] $M(NO_3)_2{\cdot}xH_2O$ (M(II) = Mn, Co, Ni, Cu, Zn)) or $Fe(TsO)_2{\cdot}6H_2O$ (TsO = *p*-tolylsulfonate), abpt, and LiTCNQ in a molar ratio of 1:2:2 were dissolved separately in 30 mL of methanol. To dissolve abpt completely, the solution was heated for a few minutes. The metal salt and abpt solutions were mixed, resulting in a clear solution, after which the LiTCNQ solution was added quickly. At room temperature black microcrystals precipitated immediately. These were collected by filtration, washed with methanol, and analyzed after drying under vacuum. Single crystals of $[Fe(abpt)_2(TCNQ)_2]$ were obtained similarly, but by starting from boiling methanolic solutions. Small black shiny cubic crystals formed immediately. Of many experiments only few afforded crystals large enough for single-crystal X-ray measurements. In some cases small amounts of $Cu(NO_3)_2{\cdot}xH_2O$ (Cu/Fe = 0.02) or $Mn(NO_3)_2{\cdot}xH_2O$ (Mn/Fe = 0.02) were added to the reaction mixture, to obtain Cu(II)- or Mn(II)-doped $[Fe(abpt)_2(TCNQ)_2]$ samples. All compounds are isostructural as determined by X-ray powder diffraction. Anal. Calcd for $[Fe(abpt)_2(TCNQ)_2]$, *viz.* $C_{48}H_{28}FeN_{20}$: C, 61.29; H, 3.00; N, 29.78; Fe, 5.94. Found: C, 60.73; H, 3.29; N, 29.75; Fe, 5.76. Anal. Calcd for $[Zn(abpt)_2(TCNQ)_2]$, *viz.* $C_{48}H_{28}N_{20}Zn$: C, 60.67; H, 2.95; N, 29.49; Zn, 6.89. Found: C, 59.58; H, 3.19; N, 28.68; Zn, 6.90.

Crystallographic Data Collection and Refinement of the Structure. The structure of $[Fe(abpt)_2(TCNQ)_2]$ has been determined at 298 K (**1**) and 100 K (**2**). Parameters of data collection and refinement are given in Table 1. X-ray data were collected for a black, tiny plate-

Table 1. Crystallographic Data for $[Fe(abpt)_2(TCNQ)_2]$ at 298 K (**1**) and 100 K (**2**)

compd	**1**	**2**
formula	$C_{48}H_{28}FeN_{20}$	$C_{48}H_{28}FeN_{20}$
molar mass, g mol^{-1}	940.73	940.73
crystal system	triclinic	triclinic
space group	$P\bar{1}$	$P\bar{1}$
T, K	298	100
a, Å	9.277(2)	9.236(2)
b, Å	9.876(3)	9.684(1)
c, Å	12.272(2)	12.137(2)
α, deg	69.52(2)	69.26(1)
β, deg	86.92(2)	87.53(2)
γ, deg	81.73(2)	82.38(1)
V, Å^3	1042.3(4)	1006.3(3)
Z	1	1
d_x, Mg/m^3	1.499	1.552
crystal size, mm	0.02 × 0.15 × 0.18	0.02 × 0.15 × 0.18
radiation (Mo Kα)[a]	0.71073	0.71073
F000	482	482
abs coeff, cm^{-1}	4.2	4.4
linear decay	4%	3%
scan width, deg	0.90 + 0.35 tan θ	0.90 + 0.35 tan θ
θ_{max}, deg	24	24
no. of total data	3491	3356
no. of unique data	3275	3145
no. of obsd data, $I > 2.5\sigma(I)$	988	1019
difabs correction range	0.74;1.19	0.80;1.17
R[b]	0.088	0.095
R_w[c]	0.071	0.055
no. of params	144	144
goodness of fit	2.30	2.73
$\Delta\varrho$ range	−0.60, 0.48	−0.79, 0.70

[a] Graphite monochromator. [b] $R = [\sum(|F_o| - |F_c|)/\sum|F_o|]$. [c] $R_w = [\sum w(|F_o| - |F_c|)^2/\sum w|F_o|^2]^{1/2}$; $w^{-1} = \sigma^2(F)$.

(4) (a) Meissner, E.; Köppen, H.; Spiering, H.; Gütlich, P. *Chem. Phys. Lett*. **1983**, *95*, 163. (b) Slichter, C. P.; Drickamer, H. G. *J. Chem. Phys*. **1972**, *56*, 2142.

(5) (a) Decurtins, S.; Gütlich, P.; Köhler, C. P.; Spiering, H.; Hauser, A. *Chem. Phys. Lett*. **1984**, *105*, 1. (b) Hauser, A.; Gütlich, P.; Spiering, H. *Inorg. Chem*. **1986**, *25*, 4245. (c) Figg, D. C.; Herber, R. H.; Potenza, J. A. *Inorg. Chem*. **1992**, *31*, 2111. (d) Hauser, A. *Chem. Phys. Lett*. **1986**, *124*, 543. (e) Decurtins, S.; Gütlich, P.; Hasselbach, K. M.; Hauser, A.; Spiering, H. *Inorg. Chem*. **1985**, *24*, 2174.

(6) Dose, E. V.; Tweedle, M. F.; Wilson, L. J.; Sutin, N. *J. Am. Chem. Soc*. **1977**, *99*, 3886.

(7) (a) Vos, G.; le Fêbre, R. A.; de Graaff, R. A. G.; Haasnoot, J. G.; Reedijk, J. *J. Am. Chem. Soc*. **1983**, *105*, 1682. (b) Vos, G.; de Graaff, R. A. G.; Haasnoot, J. G.; van der Kraan, A. M.; de Vaal, P.; Reedijk, J. *Inorg. Chem*. **1984**, *23*, 2905. (c) Vreugdenhil, W.; Haasnoot, J. G.; Kahn, O.; Theury, P.; Reedijk, J. *J. Am. Chem. Soc*. **1987**, *109*, 5272. (d) Vreugdenhil, W.; van Diemen, J. H.; de Graaff, R. A. G.; Haasnoot, J. G.; Reedijk, J.; van der Kraan, A. M.; Kahn, O.; Zarembowitch, J. *Polyhedron* **1990**, *9*, 2971. (e) Stupik, P.; Zhang, J. H.; Kwiecien, M.; Reiff, W. M.; Haasnoot, J. G.; Hage, R.; Reedijk, J. *Hyperfine Interact*. **1986**, *28*, 725. (f) Stupik, P.; Reiff, W. M.; Hage, R.; Jacobs, J.; Haasnoot, J. G.; Reedijk, J. *Hyperfine Interact*. **1988**, *40*, 343. (g) Ozarowski, A.; Shunzhong, Y.; McGarvey, B. R.; Mislankar, A.; Drake, J. E. *Inorg. Chem*. **1991**, *30*, 3167. (h) Vreugdenhil, W.; Gorter, S.; Haasnoot, J. G.; Reedijk, J. *Polyhedron* **1985**, *4*, 1769. (i) Kahn, O.; Kröber, J.; Jay, C. *Adv. Mater*. **1992**, *4*, 718. (j) Jay, C.; Grolière, F.; Kahn, O.; Kröber, J. *Mol. Cryst. Liq. Cryst*. **1993**, *234*, 255. (k) Kröber, J.; Codjovi, E.; Kahn, O.; Grolièrer, F.; Jay, C. *J. Am. Chem. Soc*. **1993**, *115*, 9810.

(8) Kahn, O.; Pei, Y.; Journaux, Y. In *Inorganic Materials*; Bruce, D. W., O'Hare, D., Eds.; Wiley: New York, 1992; p 59.

(9) Cornelissen, J. P.; van Diemen, J. H.; Groeneveld, L. R.; Haasnoot, J. G.; Spek, A. L.; Reedijk, J. *Inorg. Chem*. **1992**, *31*, 198.

(10) Geldard, J. F.; Lions, F. *J. Org. Chem*. **1965**, *30*, 318.

(11) Bozio, R.; Girlando, A.; Pecile, C. *J. Chem. Soc., Faraday Trans. 2* **1975**, *71*, 1237.

shaped crystal of approximate dimensions 0.02 × 0.15 × 0.18 mm on an Enraf-Nonius CAD4T/rotating anode system at 10 kW using graphite monochromated Mo Kα radiation (λ = 0.710 73 Å). Unit cell parameters were derived from the SET4 setting angles of 25 reflections in the range $5° < \theta < 15°$. The data were corrected for *Lp*, a small linear decay, and absorption (DIFABS[12]) and averaged into a unique data set. The 298 K structure was solved by Patterson techniques (DIRDIF-92[13]) and refined on *F* by full-matrix least-squares (SHELX-76[14]). The iron atom was refined with anisotropic displacement parameters; all other non-hydrogen atoms were refined with individual isotropic displacement parameters in view of the limited number of observed data. Hydrogen atoms were taken into account at calculated positions and their positions refined riding on their carrier atom with one common displacement parameter. Scattering factors were taken from Cromer and Mann.[15] Geometrical calculations were done with PLATON.[16] The 100 K structure was refined starting from the 298 K coordinates.

Elemental Analyses. C, H, N and metal determinations were performed by the Microanalytical Laboratory of University College, Dublin, Ireland.

X-ray Powder Diffraction. X-ray powder diagrams of the powdered coordination compounds were obtained with a Guinier-de Wolf camera using Cu Kα radiation and a nickel filter.

IR Spectra. Fourier transform infrared spectra (100−300 K) have been recorded as KBr pellets in the range 4000−250 cm^{-1} on a Bruker IFS 113V FT-IR spectrophotometer (resolution 0.5 cm^{-1}).

EPR Spectra. X-band powder EPR spectra at 9.04 GHz, 298−20 K, and microwave power of 4 mW have been obtained on a Jeol RE2x electron spin resonance spectrometer using an ESR900 continuous-flow cryostat. dpph was used as a reference.

Magnetic Measurements. Magnetic susceptibilities were measured in the temperature range 7−300 K with a fully automated Manics DSM-8 susceptometer equipped with a TBT continuous-flow cryostat and a Drusch EAF 16 NC electromagnet, operating at *ca.* 1.4 T. Data were corrected for magnetization of the sample holder and for diamagnetic contributions, which were estimated from the Pascal constants. The susceptometer was calibrated using Gd_2O_3. Magnetic susceptibility measurements between 80 and 460 K were carried out on an automated Faraday balance, described by Arbouw.[17] $HgCo(NCS)_4$ was used as a calibrant for the Faraday balance.[18]

Mössbauer Spectra. Mössbauer spectra were obtained with a constant-acceleration spectrometer, which uses a ^{57}Co in Rh source. Isomer shifts (IS) are reported relative to the NBS standard, disodium pentacyanonitrosylferrate. The measured spectra were fitted by computer, with calculated subspectra consisting of Lorentzian-shaped lines, by varying the Mössbauer parameters in a nonlinear, iterative minimization routine.

Results and Discussion

Description of the Crystal Structure of $[Fe(abpt)_2(TCNQ)_2]$ at 298 K (1) and 100 K (2). The molecular structure and the atomic numbering of the mononuclear Fe(II) cluster is depicted in Figure 1, whereas relevant bond length and bond angle information is given in Tables 2 and 3. The structure has been determined at 298 K (**1**) and 100 K (**2**). It should be noted that in **1** the compound is primarily in the high-spin state; only a fraction of low-spin iron(II) has been found to be present (*vide infra*). In the present discussion of the structure, **1** will be referred to as the high-spin state. In **2** all iron(II) atoms are in the low-spin state, although a residual amount of high-spin Fe(II) species may be present (*vide infra*). At both temperatures the space group is $P\bar{1}$. Both structures differ mainly in iron-donor atom distances and angles. The structure is isostructural with $[Cu(abpt)_2(TCNQ)_2]$.[9] The triclinic unit cell contains one mononuclear $[Fe(abpt)_2(TCNQ)_2]$ unit with the Fe(II) atom at the inversion center and a pair of centrosymmetrically related TCNQ anions. The metal ion is in a distorted octahedral environment, of which the equatorial coordination sphere is formed by the triazole-N1 and pyridyl-N1A of two abpt molecules. The Fe−N1 and Fe−N1A distances are 2.08(1) and 2.12(1) Å for **1** and 2.00(2) and 2.02(1) Å for **2**, respectively.

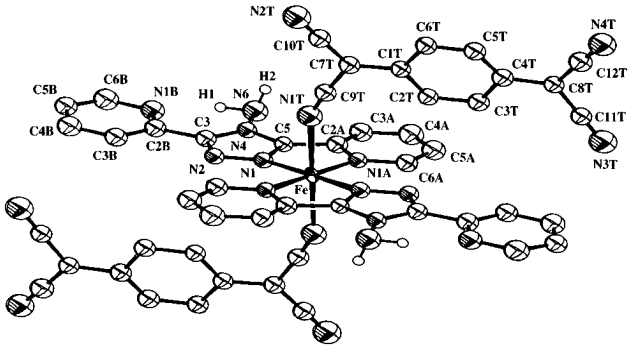

Figure 1. ORTEP[19] projection of $[Fe(abpt)_2(TCNQ)_2]$ at 298 K. Additional atoms are generated by the symmetry operation $-x, -y, -z$.

Table 2. Selected[a] Interatomic Distances (Å) for $Fe(abpt)_2(TCNQ)_2$ at 298 K(**1**) and 100 K (**2**)

	1	**2**
Fe−N1	2.08(1)	2.00(2)
Fe−N1A	2.12(1)	2.02(1)
Fe−N1T	2.16(1)	1.93(1)
N1−N2	1.36(2)	1.35(2)
N1−C5	1.32(2)	1.31(2)
N2−C3	1.30(2)	1.29(3)
N4−C3	1.35(2)	1.32(2)
N4−C5	1.37(2)	1.43(3)
N4−N6	1.39(2)	1.41(2)
C3−C2B	1.51(3)	1.54(3)
C5−C2A	1.49(2)	1.48(3)
N1A−C2A	1.34(2)	1.37(3)
N1A−C6A	1.36(2)	1.32(2)
N1B−C2B	1.31(2)	1.34(3)
N1B−C6B	1.39(2)	1.36(2)
C2A−C3A	1.36(2)	1.33(2)
C2B−C3B	1.40(2)	1.37(2)
C3A−C4A	1.39(2)	1.38(2)
C3B−C4B	1.40(3)	1.39(3)
C4A−C5A	1.37(3)	1.39(3)
C4B−C5B	1.39(3)	1.41(3)
C5A−C6A	1.37(2)	1.36(2)
C5B−C6B	1.37(2)	1.38(2)
N1T−C9T	1.13(2)	1.14(2)
N2T−C10T	1.12(2)	1.09(2)
N3T−C11T	1.14(2)	1.11(2)
N4T−C12T	1.15(2)	1.16(2)
C7T−C1T	1.42(2)	1.44(2)
C8T−C4T	1.42(2)	1.44(3)
C9T−C7T	1.43(2)	1.47(2)
C10T−C7T	1.41(2)	1.38(2)
C11T−C8T	1.42(2)	1.39(3)
C12T−C8T	1.43(2)	1.44(3)
C1T−C2T	1.41(2)	1.42(2)
C3T−C4T	1.44(2)	1.46(3)
C4T−C5T	1.38(2)	1.39(3)
C6T−C1T	1.44(2)	1.44(2)
C2T−C3T	1.40(2)	1.34(3)
C5T−C6T	1.36(2)	1.35(3)

[a] A full listing is available in the supporting information.

(12) Walker, N.; Stuart, D. *Acta Crystallogr*. **1983**, *A39*, 158.
(13) Beurskens, P. T.; Admiraal, G.; Beurskens, G.; Bosman, W. P.; García-Granda, S.; Gould, R. O.; Smits, J. M. M.; Smykalla, C. The DIRDIF program system, Technical report of the Crystallography Laboratory, University of Nijmegen, The Netherlands, 1992.
(14) Sheldrick, G. M. *SHELX76 Program for crystal structure determination*; University of Cambridge: Cambridge, U.K., 1976.
(15) Cromer, D. T.; Mann, J. B. *Acta Crystallogr*. **1968**, *A24*, 321.
(16) Spek, A. L. *Acta Crystallogr*. **1990**, *A46*, C34.
(17) Arbouw, J. W. Ph.D. Thesis, Leiden University, 1974.
(18) O'Connor, C. J.; Sinn, E.; Cukauskas, E. J.; Deaver, B. S., Jr. *Inorg. Chim. Acta* **1979**, *32*, 29.
(19) Johnson, C. K. *ORTEP*. *Report ORNL-3794*; Oak Ridge National Laboratory: Tennessee, 1965.

Table 3. Selected[a] Angles (deg) for $[Fe(abpt)_2(TCNQ)_2]$ at 298 K (**1**) and 100 K (**2**)

	1	**2**
N1−Fe−N1A	77.2(5)	80.3(6)
N1−Fe−N1T	91.5(5)	87.3(6)
N1−Fe−N1′	180.0	180.0
N1−Fe−N1A′	102.8(5)	99.7(6)
N1−Fe−N1T′	88.5(5)	92.7(6)
N1A−Fe−N1T	88.3(5)	92.2(6)
N1A−Fe−N1A′	180.0	180.0
N1A−Fe−N1T′	91.7(5)	87.8(6)
N1T−Fe−N1T′	180.0	180.0
Fe−N1−N2	135(1)	135(1)
Fe−N1−C5	113(1)	113(1)
N2−N1−C5	111(1)	112(2)
N1−N2−C3	105(1)	105(2)
C3−N4−C5	105(1)	104(2)
C3−N4−N6	132(2)	135(2)
C5−N4−N6	123(1)	121(1)
Fe−N1A−C2A	118(1)	118(1)
Fe−N1A−C6A	126(1)	127(1)
C2A−N1A−C6A	116(1)	115(2)
C2B−N1B−C6B	117(1)	114(2)
Fe−N1T−C9T	151(1)	162(1)
N2−C3−N4	113(2)	114(2)
N2−C3−C2B	123(1)	123(2)
N4−C3−C2B	124(2)	123(2)
N1−C5−N4	107(1)	106(2)
N1−C5−C2A	121(2)	122(2)
N4−C5−C2A	132(2)	133(2)
C7T−C1T−C2T	121(2)	122(2)
C7T−C1T−C6T	121(1)	122(2)
C2T−C1T−C6T	118(1)	115(2)
C5−C2A−N1A	109(1)	107(2)
C5−C2A−C3A	125(2)	127(2)
N1A−C2A−C3A	126(2)	126(2)
C3−C2B−N1B	116(1)	114(2)
C3−C2B−C3B	117(2)	118(2)
N1B−C2B−C3B	127(2)	128(2)
C1T−C2T−C3T	121(2)	124(2)
C2A−C3A−C4A	116(2)	118(2)
C2B−C3B−C4B	117(2)	117(2)
C2T−C3T−C4T	119(2)	119(2)
C3A−C4A−C5A	120(2)	118(2)
C3B−C4B−C5B	118(2)	119(2)
C3T−C4T−C5T	119(2)	118(2)
C3T−C4T−C8T	116(2)	118(2)
C5T−C4T−C8T	125(2)	124(2)
C4A−C5A−C6A	120(2)	120(2)
C4B−C5B−C6B	123(2)	119(2)
C4T−C5T−C6T	124(2)	122(2)
N1A−C6A−C5A	122(2)	123(2)
N1B−C6B−C5B	120(2)	124(2)
C1T−C6T−C5T	119(2)	122(2)
C1T−C7T−C9T	119(1)	117(2)
C9T−C7T−C10T	117(1)	119(2)
C1T−C7T−C10T	123(2)	124(2)
C4T−C8T−C11T	125(2)	124(2)
C4T−C8T−C12T	120(2)	118(2)
C11T−C8T−C12T	115(2)	117(2)
N1T−C9T−C7T	175(2)	171(2)
N2T−C10T−C7T	179(2)	179(2)
N3T−C11T−C8T	179(2)	178(2)
N4T−C12T−C8T	178(2)	177(2)

[a] Primed atoms are generated by the symmetry operations $-x, -y, -z$. A full listing is available in the supporting information.

The N1−Fe−N1A bite angle enlarges, while passing from the high-spin (77.2(5)°) to the low-spin (80.3(6)°) form. The larger bite angle in the low-spin complex is a result of the shorter Fe−N bond lengths. This effect of enlarging bite angles, while going from high-spin to low-spin state has been reported before for mononuclear iron(II) compounds with dichelating N-donating ligands.[2g,5c,20] The dihedral angle between the coordinated pyridyl group and the triazole ring is 4.2(8)° for **1** and 1.3(9)° for **2**, whereas these are 3.1(8)° for **1** and 3.8(9)° for **2**, respectively, for the noncoordinated pyridyl ring. The noncoordinating pyridyl group is oriented in such a way as to be able to form an intramolecular hydrogen bond with the amino group of the abpt ligand (See Table 4). This contributes to the approximate planarity of the abpt ligand and has been observed in other mononuclear abpt compounds.[9,21] The axial positions are occupied by two monodentate coordinating TCNQ radical anions at extremely short coordination distances, *i.e.* Fe−N1T = 2.16(1) Å for **1** and 1.93(1) Å for **2**. This is significantly shorter than the Cu−N1T distance of 2.442(5) Å found in $[Cu(abpt)_2(TCNQ)_2]$.[9] The coordinated TCNQ nitrile group shows the largest deviation from linearity, *i.e.* N1T−C9T−C7T is 175(2)° in **1** and 171(2)° in **2**, respectively. The average change in Fe(II)−donor atom bond length is 0.14 Å, which is at the lower side of the values normally encountered.[2c,g] Remarkable is the very large change in Fe−N1T distance of 0.23 Å, which is probably related to the extended π system of TCNQ, favoring increased back-bonding in the low-spin state. So far, the largest change observed in Fe−N donor atom distance on going from high-spin (HS) to low-spin (LS) state is only 0.21 Å.[20c] The $[Fe(abpt)_2(TCNQ)_2]$ units are packed in such a way that the TCNQ molecules form stacked dimers in the usually found eclipsed conformation, like the one existing in the $(TCNQ)_2^{2-}$ dimeric anion.[9,22] A view of the crystal packing is not shown here because it is completely identical to that of $[Cu(abpt)_2(TCNQ)_2]$.[9] The distance between the least-squares planes through these stacked TCNQ anion radicals, with symmetry operations (x, y, z) and $(1-x, -y, 1-z)$ shortens from 3.22 Å in the HS state to 3.15 Å in the LS state. These interplanar TCNQ−TCNQ spacings in discrete dimers fall in the range normally observed.[9,22] Clearly, the contraction of the Fe(II) coordination sphere when going from HS to LS state is accompanied by a more compact packing of the TCNQ units. It is remarkable that the tremendous shortening of the Fe−N1T distances is not completely reflected on this TCNQ−TCNQ stacking distance. This can be related to the increase in the Fe−N1T−C9T angle from 151(1)° in **1** to 162(1)° in **2**. The

Table 4. Relevant Interatomic Distances (Å) and Angles (deg) for the Hydrogen Bonding Interactions in $[Fe(abpt)_2(TCNQ)_2]$ at 298 K (**1**) and 100 K (**2**)

D−H···A	D−H	H···A	D···A	D−H···A
		compound **1**		
N6−H1···N1B	1.03(2)	1.96(2)	2.83(2)	141(1)
N6−H2···H4T[a]	0.87(2)	2.49(2)	3.25(2)	147(2)
		compound **2**		
N6−H1···N1B	1.03(2)	1.96(2)	2.83(2)	141(2)
N6−H2···N4T[a]	0.86(2)	2.39(2)	3.14(2)	146(2)

[a] Positions generated by the symmetry operation: $x, y, z-1$.

(20) (a) König, E.; Watson, K. J. *Chem. Phys. Lett.* **1970**, *6*, 457. (b) Katz, B. A.; Strouse, C. E. *J. Am. Chem. Soc.* **1979**, *101*, 6214. (c) Gallois, B.; Real, J. A.; Hauw, C.; Zarembowitch, J. *Inorg. Chem.* **1990**, *29*, 1152. (d) Baker, A. T.; Goodwin, H. A.; Rae, A. D. *Inorg. Chem.* **1987**, *26*, 3513.

(21) (a) Faulmann, C.; van Koningsbruggen, P. J.; de Graaff, R. A. G.; Haasnoot, J. G.; Reedijk, J. *Acta Crystallogr.* **1990**, *C46*, 2357. (b) García, M. P.; Manero, J. A.; Oro, L. A.; Apreda, M. C.; Cano, F. H.; Foces-Foces, C.; Haasnoot, J. G.; Prins, R.; Reedijk, J. *Inorg. Chim. Acta* **1986**, *122*, 235. (c) van Koningsbruggen, P. J.; Goubitz, K.; Haasnoot, J. G.; Reedijk, J. Manuscript in preparation.

(22) (a) Lacroix, P.; Kahn, O.; Gleizes, A.; Valade, L.; Cassoux, P. *New J. Chem.* **1984**, *8*, 643. (b) Miller, J. S.; Zhang, J. H.; Reiff, W. M.; Dixon, D. A.; Preston, L. D.; Reis, A. H., Jr.; Gebert, E.; Extine, M.; Troup, J.; Epstein, A. J.; Ward, M. D. *J. Phys. Chem.* **1987**, *91*, 4344. (c) Humphrey, D. G.; Fallon, G. D.; Murray, K. S. *J. Chem. Soc., Chem. Commun.* **1988**, 1356. (d) Lau, C.-P.; Singh, P.; Cline, S. J.; Seiders, R.; Brookhart, M.; Marsh, W. E.; Hodgson, D. J.; Hatfield, W. E. *Inorg. Chem.* **1982**, *21*, 208.

Table 5. Least-Squares Fit Mössbauer Data for $[Fe(abpt)_2(TCNQ)_2]$[a]

	low-spin state			high-spin state					
T (K)	IS (mm s^{-1})	ΔE_Q^{1-2} (mm s^{-1})	relative area (%)	IS (mm s^{-1})	ΔE_Q^{1-5} (mm s^{-1})	relative area (%)	IS (mm s^{-1})	ΔE_Q^{1-6} (mm s^{-1})	relative area (%)
120	0.76	0.69	100						
150	0.75	0.69	100						
180	0.74	0.69	100						
210	0.73	0.69	97	1.41	2.06	3			
225	0.72	0.69	94	1.37	2.00	6			
240	0.70	0.70	91	1.35	1.99	9			
255	0.69	0.73	85	1.29	1.93	15			
270	0.66	0.73	83	1.25	1.92	17			
285	0.54	0.54	67	1.15	1.76	33			
300				1.14	1.80	84	0.44	0.39	16
315				1.15	1.85	92	0.44	0.43	8
330				1.16	1.90	92	0.43	0.44	8
360				1.17	1.95	93	0.41	0.43	7

[a] IS = isomer shift, ΔE_Q = quadrupole splitting relative to the numbered singlets.

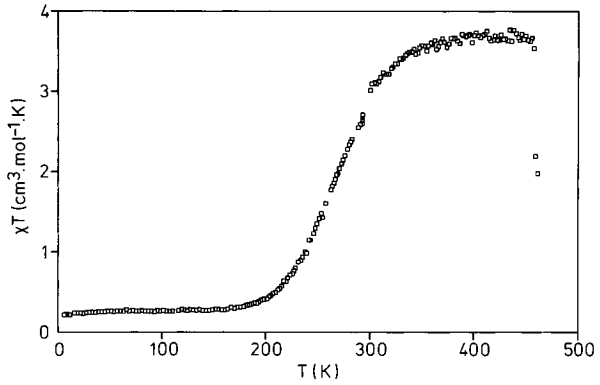

Figure 2. χT vs T curve (□) (T = 7−460 K) for $[Fe(abpt)_2(TCNQ)_2]$. Points at 470 K indicate sample decomposition.

structure is stabilized further by one weak and one strong N−H···N hydrogen bond, data of which are summarized in Table 5.

Magnetic Susceptibility Measurements. The magnetic susceptibility data recorded for $[Fe(abpt)_2(TCNQ)_2]$ in the temperature range 7−460 K provide evidence for an $S = 2$ (HS) ↔ $S = 0$ (LS) spin-crossover behavior (See Figure 2). The product of the molar magnetic susceptibility (χ) and the temperature (T) is 3.70 cm^3 mol^{-1} K at 450 K, which is consistent with the effective magnetic moment $\mu_{eff} = 5.44\mu_B$, corresponding to a quintet spin state. Upon lowering the temperature, χT attains a value of 0.25 cm^3 mol^{-1} K ($\mu_{eff} = 1.41\mu_B$) at 7 K. This is very close to the value expected for a singlet spin state, indicating that the spin-crossover is almost complete. Although, this residual paramagnetism may be interpreted as indicative of about 7% of high-spin Fe(II) species, its presence has not been detected by Mössbauer spectroscopy (*vide infra*). On the other hand, in the EPR spectra (*vide infra*), signals due to small $TCNQ^{\bullet-}$ radical anion impurities have been observed, which may also result in paramagnetism at low temperatures. Further, the μ_{eff} value of $5.44\mu_B$ at 450 K is at the upper limit of the values normally encountered for high-spin Fe(II); this excludes the presence of LS Fe(II) at this temperature. Yet the Mössbauer spectrum (*vide supra*) at 330 K shows an asymmetry of the Fe(II) HS lines. This asymmetry may be due to high-spin Fe(III) impurity, which could at the same time explain part of the enhanced μ_{eff} value of $1.41\mu_B$ at 7 K.

The transition temperature of this gradually proceeding spin transition is about 280 K. The transition does not show any hysteresis, since the χT *vs* T curves recorded at decreasing and increasing temperatures are identical. Magnetic coupling within the dimerized TCNQ units is very strong, resulting in a diamagnetic behavior over the whole temperature range studied. Indeed, it has frequently been observed that the antiferromagnetic exchange coupling within a stacked TCNQ pair is generally very large due to the strong π interaction.[22a,23] The magnetic data recorded for the X-ray isomorphous $[Zn(abpt)_2(TCNQ)_2]$ show that the χT value remains relatively constant at a value of 0 cm^3 mol^{-1} K over the whole temperature range. For the compounds containing the paramagnetic metal(II) ions Mn, Co, Ni, and Cu, the χT *vs* T curves follow the Curie Law, corresponding to the respective high-spin metal(II) energy states (data not shown).

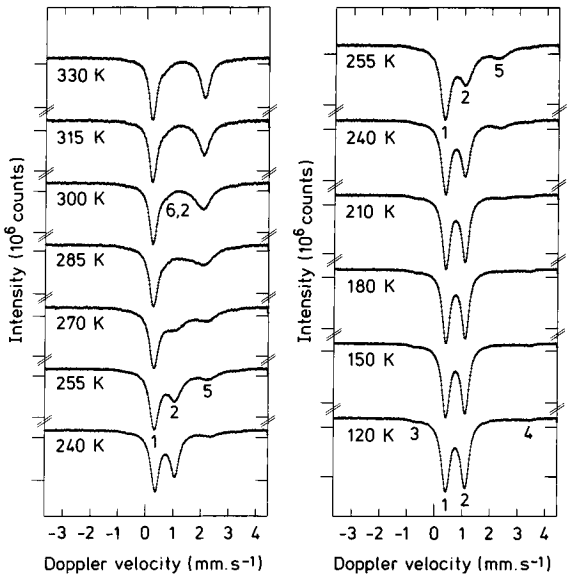

Figure 3. Selected ^{57}Fe Mössbauer spectra of $[Fe(abpt)_2(TCNQ)_2]$.

Mössbauer Spectroscopy. ^{57}Fe Mössbauer spectroscopy measurements have been performed in the temperature range 360−120 K. Representative spectra are presented in Figure 3. From the spectrum at T = 120 K, it is seen that besides the central electric quadrupole doublet small additional contributions to the spectrum are present at Doppler velocities of about −0.7 and 3.3 mm s^{-1}. These very small spectral contributions (absorptions 3 and 4) have been ignored in the analyses of the measured spectra. As shown in Figure 3, the central doublet with a small quadrupole splitting (at T = 120 K) is gradually

(23) (a) Miller, J. S.; Calabrese, J. C.; Harlow, R. L.; Dixon, D. A.; Zhang, J. H.; Reiff, W. M.; Chittipeddi, S.; Selover, M. A.; Epstein, A. J. *J. Am. Chem. Soc.* **1990**, *112*, 5496. (b) Schwartz, M.; Hatfield, W. E. *Inorg. Chem.* **1987**, *26*, 2823.

changing into a doublet with a much larger splitting (at $T =$ 360 K) with increasing temperature. These doublets can be ascribed to the LS and the HS state of Fe(II), respectively. In that case the spin-transition temperature is determined to occur at about 280 K, in agreement with the results of the magnetic susceptibility measurements, presented in Figure 2. In the spin-transition region, the LS absorption line and to some extent the HS lines show a significant broadening and an increasing asymmetry of the HS lines. Although distinct spectra for both spin states are observed, the behavior is characteristic for relaxation effects, where the rate constant for the spin-conversion process (denoted as k_{LH}) is about equal to the nuclear Larmor precession frequency for the ^{57}Fe nucleus (denoted as ω_n).[24] The spectra presented in Figure 3 have been analyzed using single Lorentzian-shaped lines, and the isomer shift (IS) values and quadrupole splitting (ΔE_Q) values are deduced from the individual line positions and listed in Table 5 together with the spectral contributions (in percent). It should be noted that the fitting procedure applied does not account for the relaxation effects, from which result part of the line broadening and asymmetry of the absorptions. A more correct and detailed interpretation of the Mössbauer data may be obtained using the stochastic theory of line shape of Blume.[25] Therefore, it would be worthwhile to subject the present Mössbauer data to a line shape analysis that will eventually produce values of rate constants for the dynamic spin state interconversion process. Consistent with the magnetic susceptibility measurements, no hysteresis in the low-spin/high-spin transition has been observed by Mössbauer spectroscopy.

However, the present analyses of the spectra measured at 315, 330, and 360 K indicate that a residual spectral contribution had to be included in the fitting procedure; this contribution is listed in the last three columns of Table 5. This impurity (absorption 6) may be due to HS Fe(III), which is expected to have a small ΔE_Q. This is further supported by the observed asymmetry in the Fe(II) LS lines at 120 K. As the Debye−Waller factors for Fe(II) and Fe(III) are far different, a good estimate of the amount of Fe(III) is not possible. It is expected that an impurity of about 3% already could give rise to such "perturbed" Mössbauer spectra. This also contributes to the residual magnetism at low temperatures and the high μ_{eff} at 450 K.

Infrared Spectroscopy. The FT-IR spectra of the X-ray isomorphous series of compounds $[M(abpt)_2(TCNQ)_2]$ (M(II) = Mn, Fe, Co, Ni, Cu, Zn) are all very similar. The absorption at 828 cm^{-1} clearly indicates the presence of solely the uninegative $TCNQ^{\bullet -}$ radical ion.[26] The characteristic strong absorption around 2190 cm^{-1} (ν_{CN}) is split; this splitting can be explained by the fact that the nitrile groups are inequivalent, *i.e.* the presence of coordinating, noncoordinating, and CN groups involved in hydrogen bonding. The positions of the ν_{CN} absorptions are listed in Table 6. Absorptions B and C do not show a large change in frequency upon changing the metal ion or the spin state. These absorptions might be assigned to the asymmetric (B) and symmetric (C) vibrations of the noncoordinating CN groups of TCNQ. Absorptions A and D could be due to the two cyano groups in the closest vicinity of the metal(II) ion coordination sphere (one of these being the coordinated TCNQ nitrile group), since these nitriles will mostly be influenced by a change in metal ion or spin state. Figure 4 shows the position of the ν_{CN} absorptions as function of the crystal field stabilization energy (CFSE) in the ideal case of an assumed

Table 6. FT-Infrared Spectroscopy Data for the ν_{CN} Absorption (cm^{-1}) for $[M(abpt)_2(TCNQ)_2]$ (M(II) = Mn, Fe, Co, Ni, Cu)

M(II)	d^n	CFSE (Dq)	ν_{CN} (A)	ν_{CN} (B)	ν_{CN} (C)	ν_{CN} (D)
Mn	d^5	0	2185		2159	2149
Fe (HS)	d^6	−4	2187	2183	2159	2150
Cu	d^9	−6	2185	2180	2158	2154
Co	d^7	−8	2188	2184		2156
Ni	d^8	−12	2189	2184		2160
Fe (LS)	d^6	−24	2198	2186	2164	2169

[a] A, B, C, and D represent the various absorptions.

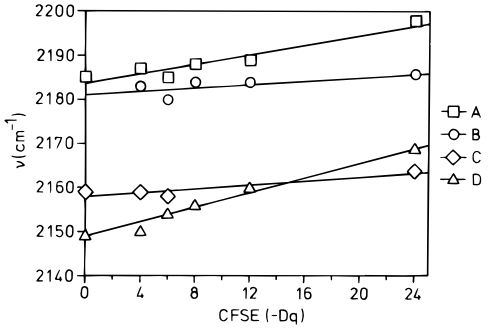

Figure 4. Plot of the ν_{CN} absorptions as a function of the crystal field stabilization energy (CFSE) for assumed O_h symmetry. The lines drawn are meant as a guide for the eye. The metal ions are as listed in Table 6.

O_h symmetry around the metal(II) ion. All absorptions show a shift to higher frequencies as a function of the CFSE, which is a known behavior.[27] It should be noted that the agreement for Cu(II) is less good, apparently due to its Jahn−Teller distorted geometry. The FT-IR spectra recorded for $[Fe(abpt)_2(TCNQ)_2]$ in the temperature range 100−300 K monitor the effect of the spin-crossover on the frequency and intensity of the ν_{CN} absorptions. Clearly, the series of ν_{CN} vibrations are a fingerprint for Fe(II) HS (in Figure 5 denoted as absorptions A^1 and D^1) and LS states (absorptions A^2 and D^2). Moreover, the spectra recorded at various temperatures represented in Figure 5 confirm the coexistence of HS and LS states.

EPR Spectroscopy. The thermally induced HS ↔ LS transition of $[Fe(abpt)_2(TCNQ)_2]$ has been followed by variable-temperature X-band powder EPR spectroscopy by using the Cu(II)- and Mn(II)-doped Fe(II) species. The spectra recorded at various temperatures for Cu(II)- and Mn(II)-doped Fe(II) compounds are represented in Figures 6 and 7, respectively. Although the $TCNQ^{\bullet -}$ radical anions are dimerized, yielding diamagnetic entities, a narrow signal at $g = 2.00$ remains visible in all spectra; this signal is attributed to small nondimerized $TCNQ^{\bullet -}$ impurities.[28] Because of the completeness of the transition, it is likely that the host lattice becomes essentially diamagnetic below T_c, whereas it is paramagnetic above T_c. In the paramagnetic phase the EPR spectra are poorly resolved due to exchange broadening, but this changes dramatically after the spin transition to spectra with sharp and distinct features. However it cannot be excluded that relaxation effects play an important role. Further investigations on this could be very useful.

Above T_c, the Cu(II)-doped Fe(II) species shows a broad signal with $g_\perp = 2.09$ and $g_\parallel = 2.25$ and hyperfine structure ($A_\parallel = 180$ G), in agreement with a copper(II) ion in an elongated tetragonal environment.[29] In contrast, at T_c and below, the spectrum becomes better resolved and now even shows super-

(24) (a) Adler, P.; Spiering, H.; Gütlich, P. *Inorg. Chem.* **1987**, *26*, 3840. (b) König, E. *Struct. Bonding* **1991**, *76*, 51.
(25) Blume, M. *Phys. Rev.* **1968**, *174*, 351.
(26) Lunelli, B.; Pecile, C. *J. Chem. Phys.* **1970**, *52*, 2375.
(27) Gans, P. In *Vibrating molecules*; Chapman and Hall LTD: London, 1971; p 179.
(28) Inoue, M.; Inoue, M. B. *Inorg. Chem.* **1986**, *25*, 37.
(29) Hathaway, B. J.; Billing, D. E. *Coord. Chem. Rev.* **1970**, *5*, 143.

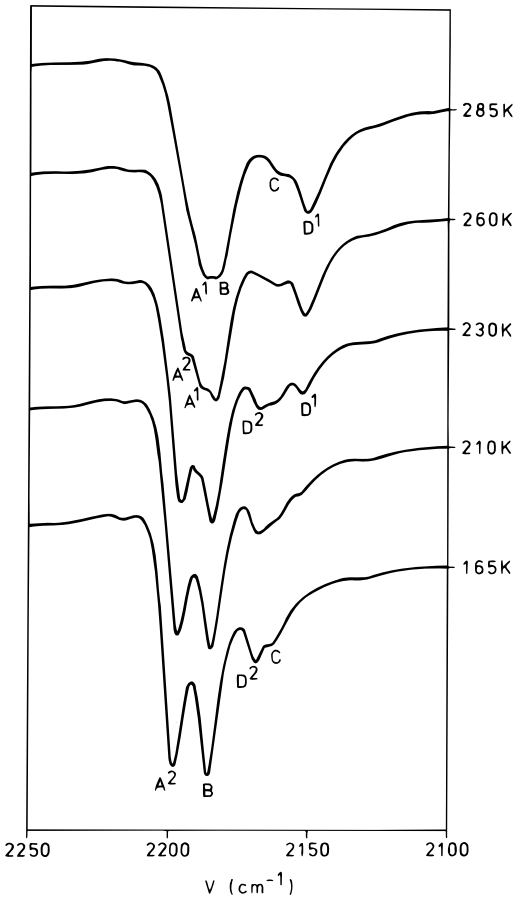

Figure 5. Selected FT-IR spectra in the CN stretch region of $[Fe(abpt)_2(TCNQ)_2]$.

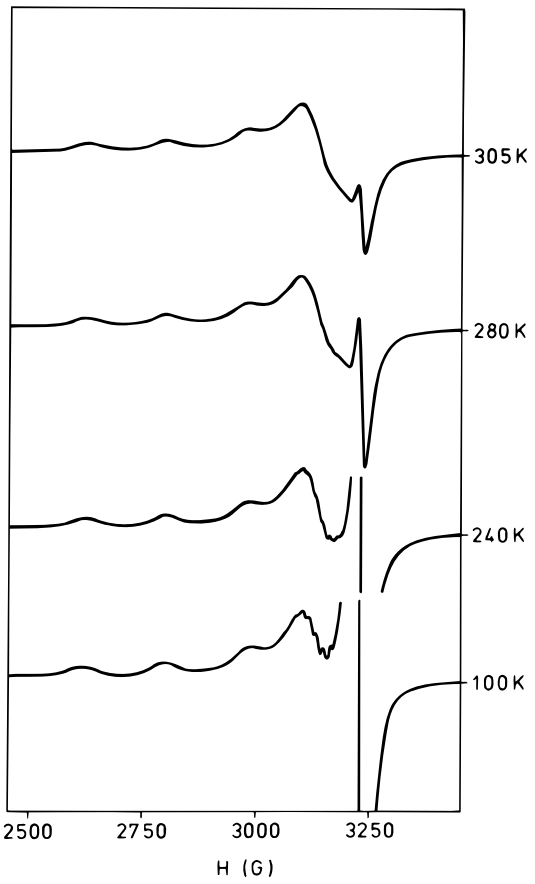

Figure 6. Selected X-band powder EPR spectra of Cu(II)-doped $[Fe(abpt)_2(TCNQ)_2]$.

hyperfine structure ($A_{N||} = 16$ G). The superhyperfine structure splits each line into nine components, due to the coupling of the unpaired electron of copper(II) with the four abpt nitrogen atoms in the equatorial coordination sphere. Above T_c, the Mn(II)-doped Fe(II) compound shows a very broad signal at $g = 2.00$. The spectrum sharpens at T_c to give a clearly resolved spectrum corresponding to a magnetically isolated Mn(II) ion in a tetragonal environment.[30] The signal is split by the zero-field splitting, yielding additional signals at $g = 1.6$ and $g = 5.5$ and six hyperfine lines ($A_{||} = 80$ G) are clearly visible on both signals. As might be expected, the EPR spectra of the Mn(II)- and Cu(II)-doped diamagnetic isostructural Zn(II) compound (data not shown) are similar to those of the doped Fe(II) species at temperatures below T_c.

These results show a striking similarity to those obtained for the also tetragonally coordinated $[Fe(btr)_2(NCS)_2]H_2O$ compound and its Cu and Mn dopes described by Vreugdenhil et al.[7c] and extensively investigated by Ozarowski et al.[7g]

Concluding Remarks

A unique new type of Fe(II) spin-crossover compound has been reported. The compound represents the first example of TCNQ radical anions coordinating monodentately to Fe(II). In fact, coordination of TCNQ rarely occurs; the molecule has strong electron affinity, which is caused by the electron-withdrawing capacity of the four cyano groups. Therefore, TCNQ easily absorbs an electron and forms the radical anion $TCNQ^{\bullet -}$. In several cases coordination of $TCNQ^{\bullet -}$ to monovalent metal ions has been found.[22c,31] However, coordination to divalent metal ions is rarely observed. Coordination of TCNQ to Cu(II) and Ni(II) has been found in $ML(TCNQ)_2$ (LH_2 = the tetra-Schiff base macrocycle resulting from the 2/2 condensation of 1,3-diaminopropane and 2,6-diformyl-4-methylphenol).[22a] Very recently, $[Mn^{II}(tpa)(TCNQ)(CH_3OH)](TCNQ)_2 \cdot CH_3CN$ (tpa = tris(2-pyridylmethyl)amine) has been reported.[32] The present series of six isomorphous compounds $[M^{II}(abpt)_2(TCNQ)_2]$, where M(II) = Mn, Fe, Co, Ni, Cu, and Zn,[9] reported here is unique in this respect. Besides its strong electron-accepting properties, the unfavorability of TCNQ toward coordination is also related to crystal packing efficiency considerations. Usually the TCNQ moieties have a tendency to form segregated stacks of cations and anions, in which the TCNQ−TCNQ stacking distances are frequently not equidistant, giving rise to the formation of di-, tri-, tetra-, and pentamers.[22d] Stacking interactions in TCNQ compounds definitely lead to more stable solid compounds, which are more easily formed. Indeed, in all compounds known to contain N-coordinating TCNQ radical anions, the TCNQ units are present in the crystal lattice in such a way as to be able to form at least stacked dimers.[9,22a,c,31,32] Apparently, the TCNQ molecules only coordinate in cases in which the formation of stacks is possible. A review article describing the structural and electronic features

(30) Dowsing, R. D.; Nieuwenhuijse, B.; Reedijk, J. *Inorg. Chim. Acta* **1971**, *5*, 301.

(31) (a) Ballester, L.; Barral, M. C.; Gutiérrez, A.; Jiménez-Aparicio, R.; Martinez-Muyo, J. M.; Perpiñan, M. F.; Monge, M. A.; Ruíz-Valero, C. *J. Chem. Soc., Chem. Commun.* **1991**, 1396. (b) Shields, L. *J. Chem. Soc., Faraday Trans. 2* **1985**, *81*, 1. (c) Grossel, M. C.; Evans, F. A.; Hriljac, J. A.; Morton, J. R.; LePage, Y.; Preston, K. F.; Sutcliffe, L. H.; Williams, A. J. *J. Chem. Soc., Chem. Commun.* **1990**, 439.

(32) Oshio, H.; Ino, E.; Mogi, I.; Ito, T. *Inorg. Chem.* **1993**, *32*, 5697.

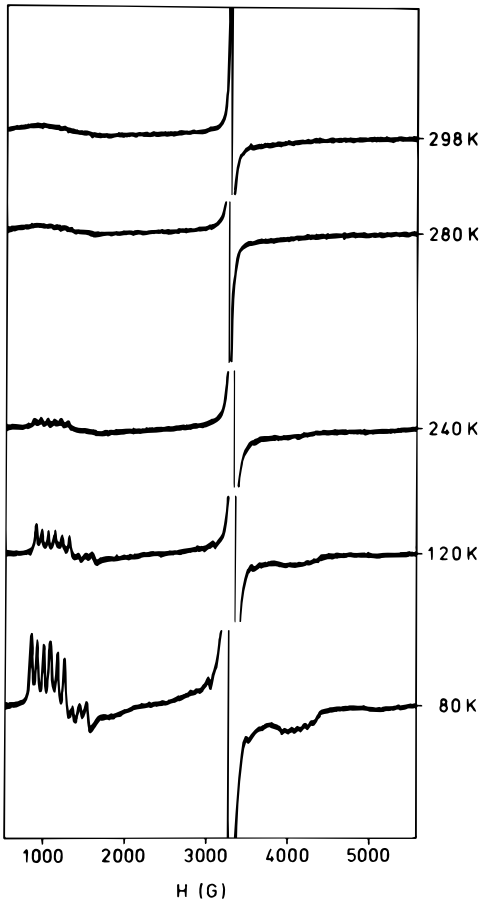

Figure 7. Selected X-band powder EPR spectra of Mn(II)-doped $[Fe(abpt)_2(TCNQ)_2]$.

of metal compounds containing TCNQ and related polynitrile π acceptors has very recently become available.[33]

Spin-crossover behavior has frequently been observed for Fe(II) ions coordinated by two didentate chelating nitrogen-donating ligands, together with two monodentately coordinating nitrogen-donating ligands.[2,5c,20] In these cases, the monodentate ligands are generally in a *cis* configuration; a *trans* geometry has so far only been found for the two-dimensional compounds $[FeX_2(btr)_2](H_2O)$ (X = NCS,[7c,d] NCSe;[7g] btr = 4,4′-bis(1,2,4-triazole)). The *trans* orientation of the TCNQ radical anions in the present compound is directly related to the crystal packing efficiency considerations for the TCNQ radical anions, as mentioned above.

The compound $[Fe(abpt)_2(TCNQ)_2]$ is particularly interesting, since it exhibits a reversible spin-crossover very close to room temperature. No hysteresis could be detected. It is known that, in solid systems, the spin-crossover phenomenon is not uniquely of molecular origin; the existence of interactions between the molecular units results in a more or less pronounced cooperative effect. This cooperative effect generally accepted to be closely related to the occurrence of hysteresis.[2c] Several attempts have been undertaken to describe the mechanism accounting for this cooperativity.[2c] However, an adequate model has not yet been found. Several authors even suggested the possibility of hysteresis at a purely molecular scale, *i.e.* for molecules having no interaction.[34] Clearly, the factors accounting for hysteresis occurring in the spin transition are not yet completely understood. The absence of hysteresis for the present compound can therefore at this stage not be rationalized, and further research will be required.

Clearly, $[Fe(abpt)_2(TCNQ)_2]$ is the first example of an up to now unknown family of spin-transition compounds. Because of its interesting physical properties and possible applications in molecular electronics, the research on this type of spin-crossover compound will be explored further, *i.e.* by changing the 1,2,4-triazole ligand or the TCNQ derivative. A change in the coordination environment of the Fe(II) ion is expected to influence directly the spin-crossover behavior. Such studies may yield Fe(II) compounds showing a more abrupt spin transition, perhaps also taking place with hysteresis.

In the present series of isostructural compounds of general formula $[M^{II}(abpt)_2(TCNQ)_2]$ (M(II) = Mn, Fe, Co, Ni, Cu, Zn),[9] in spite of the short M−N(TCNQ) distances, no magnetic coupling could be observed between the radical anion and the paramagnetic metal(II) ion. From X-ray structure determinations for the Cu(II)[9] and Fe(II) analogues, it became evident that dimerization of the radical anions occurs. Due to this dimerization, a very strong antiferromagnetic coupling occurs within the stacked TCNQ pair. This large diamagnetic unit apparently does not allow significant superexchange between the parmagnetic metal(II) ions. Consequently, the magnetic behavior of the compounds follows the Curie law for the corresponding metal(II) ions.

It would be highly interesting to "decouple" or to diminish the magnetic coupling within dimerized TCNQ units. In that case, stacking interactions between the radical anions should be prevented. This may be achieved upon using substituted TCNQ derivatives, such as 2,5-dimethyl-7,7′,8,8′-tetracyanoquinodimethane (DMTCNQ). This appears particularly interesting in the case of Fe(II). In that way, compounds with an up to now not observed combination of magnetic phenomena ((direct) exchange interactions and HS ↔ LS spin crossover) might be obtained. Further studies along this line are in progress and are expected to yield compounds with a new magnetic behavior.

Acknowledgment. The authors would like to thank the "Werkgroep Fundamenteel Materialen Onderzoek" (WFMO) for financial support. This work was supported in part (A.L.S.) by the Netherlands Foundation of Chemical Research (SON) with financial aid from the Netherlands Foundation for Scientific Research (NWO). Financial support by the European Union, allowing regular exchange of preliminary results with several European colleagues (D. Gatteschi, P. Gütlich, and O. Kahn), under Contract ERBCHRXCT920080, is thankfully acknowledged. Mr. G. A. van Albada is thanked for assistance with the FT-IR measurements.

Supporting Information Available: Complete listings of bond lengths and angles and positional parameters and figure of the crystal packing (15 pages); listings of structure factors (7 pages). This material is contained in many libraries on microfiche, immediately follows this article in the microfilm version of the journal, can be ordered from the ACS, and can be downloaded from the Internet; see any current masthead page for ordering information and Internet access instructions.

JA943960S

(33) Kaim, W.; Moscherosch, M. *Coord. Chem. Rev.* **1994**, *129*, 157.

(34) Bolvin, H.; Kahn, O.; Vekhter, B. *New J. Chem.* **1991**, *15*, 889.